Large Effect on Borane Bond Dissociation Energies Resulting from Coordination by Lewis Bases

Paul R. Rablen

Contribution from the Department of Chemistry, Swarthmore College, 500 College Avenue, Swarthmore, Pennsylvania 19081-1397

Received March 18, 1997[⊗]

Abstract: Ab initio molecular orbital calculations at the G-2 and CBS-4 levels of theory were used to determine homolytic bond dissociation energies (BDE's) for the B−H bonds in a series of donor−acceptor complexes of borane. The B−H bonds of four-coordinate boron were found to be weaker than those of three-coordinate boron. The effect of complexation on BDE varied from very small, in the cases of NH_3 and H_2O, to as much as 30−50 kcal/mol, in the cases of formaldehyde, CO, and HCN. The BDE's were not found to correlate with the strength of coordination. However, they were closely correlated with the degree to which spin density in the radical was delocalized away from boron and onto the associated Lewis base. The presence of either a π system or, to some extent, a second-row element such as phosphorus or sulfur promoted such delocalization. Delocalization of spin density onto carbon appeared to be particularly favorable, and to correlate with particularly low B−H BDE's. The BDE's in 4-coordinate complexes of borane with various larger ligands, including typical ethers and amines, followed patterns almost identical with those in the smaller species, and could be understood according to the same principles.

Introduction

Boranes play an important role in synthetic chemistry and have received extensive attention in the chemical literature.[1−3] Accurate knowledge of the thermodynamics of bond dissociation would serve as a useful framework from which to build a detailed and quantitative understanding of borane reactivity and mechanism. However, experimental bond dissociation energies (BDE's) are often difficult to obtain.[4] For instance, the presence of multiple isomers and uncertainty regarding the true coordination numbers of borane species contribute to ambiguity in the interpretation of experimental results.[5] Furthermore, bomb calorimetry, which has been used to derive BDE's, yields information only about average bond energies.[4] However, it is the sequential BDE's that are most relevant to reaction chemistry, and it has been shown that the two are often quite different.[6,7]

Ab initio molecular orbital (MO) methods are now able to provide BDE's with chemically useful accuracy and high reliability.[8] Furthermore, these methods directly yield the sequential BDE's rather than the average bond energies, and no ambiguity exists regarding multiple isomers or coordination states. Given the need for quantitative thermodynamic information about bond dissociation in boranes and the suitability of computational methodology for answering such questions, we have embarked on a systematic study of calculated borane BDE's.

In a previous investigation the BDE's of the B−H bonds in trivalent boron species were found to be remarkably insensitive to structural variation.[6] The degree of alkyl substitution at boron, the electronegativity of substituents bound to boron, and the π-donating ability of substituents all exerted almost no influence, such that the B−H BDE invariably fell within the range 108 ± 4 kcal/mol. Even conjugation did not significantly modify the BDE's, except in the unusual case of boracyclopentadiene. Methyl B−C bonds were found to have exactly the same pattern of behavior as the B−H bonds, and almost exactly the same magnitudes.

Being Lewis acids themselves, boranes frequently exist as complexes with Lewis bases. Consequently, the BDE's of tetracoordinate boron species complexed in this manner are generally more relevant to solution chemistry than are the BDE's of isolated tricoordinate boron species. Not only is the usual solution condition of a borane more accurately described by a coordinated state than by a strictly trivalent state, but coordination can play a key role in the reactivity or selectivity of a borane reagent. For instance, coordination of trivalent boron with a ketone to form a tetracoordinate intermediate is thought to provide the enantioselectivity of the "chemzyme" reduction procedures developed by Corey.[9] The coordinating behavior of boron is also known to play a role in the inhibition of certain enzymes by boron-containing species such as thienodiazaborine and benzodiazaborine. These two compounds both inhibit the bacterial enzyme enoyl reductase, which is the target of the antitubercular drug isoniazid. Each of these inhibitors forms a covalent bond between its trivalent boron center and an oxygen atom of NAD^+ when bound to enoyl reductase, generating a tetracoordinate boron species.[10]

[⊗] Abstract published in *Advance ACS Abstracts,* August 15, 1997.

(1) Pelter, A.; Smith, K.; Brown, H. C. *Borane Reagents*; Academic Press: New York, 1988.

(2) Brown, H. C. *Organic Syntheses via Boranes*; Wiley: New York, 1975.

(3) Brown, H. C. *Boranes in Organic Chemistry*; Cornell University Press: Ithaca, NY, 1972.

(4) Odom, J. D. In *Comprehensive Organometallic Chemistry*; Wilkinson, G., Stone, F. G. A.; Abel, E. W., Eds.; Pergamon Press: Oxford, 1982; Vol. 1, p 257.

(5) (a) Cooper, W. J.; Masi, J. F. *J. Phys. Chem.* **1960**, *64*, 682−683. (b) McCoy, R. E.; Bauer, S. H. *J. Am. Chem. Soc.* **1956**, *78*, 2061−2065. (c) Bennett, J. E.; Skinner, H. A. *J. Chem. Soc.* **1962**, 2150−2153. (d) Steele, W. C.; Nichols, L. D.; Stone, F. G. A. *J. Am. Chem. Soc.* **1962**, *84*, 1154−1158. (e) Ruscic, R.; Mayhew, C. A.; Berkowitz, J. *J. Chem. Phys.* **1988**, *88*, 5580−5593.

(6) Rablen, P. R.; Hartwig, J. F. *J. Am. Chem. Soc.* **1996**, *118*, 4648−4653.

(7) Rablen, P. R.; Hartwig, J. F.; Nolan, S. P. *J. Am. Chem. Soc.* **1994**, *116*, 4121−4122.

(8) Pople, J. A.; Luke, B. T.; Frisch, M. J.; Binkley, J. S. *J. Phys. Chem.* **1985**, *89*, 2198−2203.

(9) Corey, E. J.; Bakshi, R. K. *Tetrahedron Lett.* **1990**, *31*, 611−614. Corey, E. J.; Shibata, S.; Bakshi, R. K. *J. Org. Chem.* **1988**, *53*, 2861−2863. Corey, E. J.; Bakshi, R. K.; Shibata, S.; Chen, C.-P.; Singh, V. K. *J. Am. Chem. Soc.* **1987**, *109*, 7925−7926. Corey, E. J.; Bakshi, R. K.; Shibata, S. *J. Am. Chem. Soc.* **1987**, *109*, 5551−5553.

S0002-7863(97)00870-6 CCC: $14.00

The effect of coordination received limited examination in our previous study, through inclusion of diborane and aminoborane complex as examples, both of which showed B−H BDE's weakened by approximately 5 kcal/mol relative to free borane.[6] This fairly small perturbation was attributed to the change in hybridization at boron. However, further exploration revealed that borane BDE's are highly sensitive to the nature of the coordinating ligand, in stark contrast to their insensitivity to structural variation within the tricoordinate motif. While the B−H bonds in diborane and borazane are only slightly weaker than in borane, many other coordinating Lewis bases dramatically reduce the BDE's. Here we extend our investigation of boranes to include the effects of coordination by electron pair donors in a systematic fashion. The effects themselves are quite pronounced, and consequently are of substantial interest in their own right. In addition, we have attempted to use the wave functions derived from ab initio calculations to gain insight into why some ligands exert such a profound influence, while others exert almost none at all.

Results and Discussion

Computational Methodology. Theoretical methods are currently available that provide molecular energies with exceptional accuracy.[8] One of the most reliable and extensively tested is Pople's G-2 procedure, which is effectively QCISD(T)/6-311+G(3df,2p) and reproduces atomization energies with an accuracy of ±1 kcal/mol.[11,12] Accurate sequential BDE's are accessible by calculation of the G-2 energies of closed shell molecules and of the corresponding open shell species derived by bond cleavage. However, G-2 is very demanding of computational resources, and an alternative approach is necessary to obtain similarly accurate BDE's for larger molecules. The CBS-4 method recently developed by Petersson and Ochterski consumes far less computer time and disk space, and demonstrates an accuracy only modestly diminished from G-2 theory.[13−17] A single-point Hartree−Fock calculation with a very large basis set (6-311+G(3d2f,2df,p)) at the HF/3-21G* optimized geometry serves as the foundation of the CBS-4 calculation. Correction for electron correlation is made by using subsequent MP2 and MP4(SDQ) calculations with much smaller basis sets followed by an extrapolation to the complete basis set limit.[13,14] While remarkably economical, the CBS-4 procedure still reproduces the atomization energies of the 55 molecules in the G-2 test set with an average absolute error of only 1.9 kcal/mol.[16,17]

Previous work has shown excellent and consistent agreement between BDE's calculated by using these procedures and the limited experimental data available.[6,7] For instance, the average BDE for BH_3 is 89 kcal/mol experimentally, and was calculated at 89.6 and 89.1 kcal/mol by the G-2 and CBS-4 methods, respectively. Furthermore, the economical CBS-4 procedure was found to yield BDE's only 1−2 kcal/mol different from those obtained by using the far costlier G-2 procedure in all cases where both calculations were feasible. On the basis of this earlier success with closely related compounds, G-2 and CBS-4 are expected to yield similarly accurate BDE's in the present investigation.

Table 1. G-2 and CBS-4 Bond Dissociation Enthalpies (kcal/mol)

	0 K		298 K	
bond	G-2	CBS-4	G-2	CBS-4
BH_2-H	105.2	104.0	106.6	105.5
B_2H_5-H	100.2	98.7	101.9	100.3
H_3NBH_2-H	102.1	101.1	103.6	102.6
H_2OBH_2-H	104.4	103.0	105.8	104.5
H_3PBH_2-H	92.6	90.5	93.9	91.9
$OCBH_2-H$	78.6	75.5	79.9	76.8
H_2BCO-H	22.4	19.0	23.5	20.2
$H_2BC(=O)-H$	52.4	50.2	53.5	51.2
$COBH_2-H$	105.4	106.7	105.6	107.2
H_2BOC-H	70.4	67.7	72.1	69.0
H_2COBH_2-H	56.1	54.0	57.3	55.4
H_2BOCH_2-H	98.8	97.7	100.3	99.2
$HCNBH_2-H$	72.8	66.5	74.0	67.7
$H_2BNCH-H$	93.8	92.0	95.2	93.5
$HNCBH_2-H$	75.2	73.1	76.4	74.4
$H_2BCNH-H$	59.3	59.0	60.7	60.4
$H_2BC(=NH)-H$	67.8	65.8	69.3	67.3
$(CH_3)_2OBH_2-H$		102.4		103.9
CH_3CNBH_2-H		72.3		73.4
$(CH_3)_2SBH_2-H$		94.0		95.5
$(CH_3)_2COBH_2-H$		64.2		65.5
$(CH_3)_3NBH_2-H$		101.1		102.6
$(CH_3)_3PBH_2-H$		91.3		92.8
$(CH_3)_2SOBH_2-H$		99.0		100.5
$THF-BH_2-H$		101.9		103.5
$pyridine-BH_2-H$		67.6		68.8

Effect of Coordination on the B−H BDE of Borane. Table 1 lists the B−H BDE's calculated at the G-2 and CBS-4 levels for a series of boron species. The absolute molecular energies are provided in Table A in the Supporting Information.

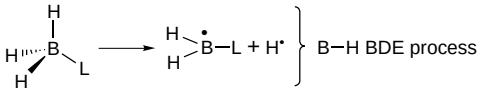

Zero-point vibrational energy corrections constitute an integral part of the CBS-4 and G-2 procedures, so that the BDE's represent enthalpies at 0 K.[11,12,16,17] The calculated vibrational frequencies also facilitate thermodynamic corrections yielding enthalpies at 298 K, which are reported in the last two columns.

Coordination of borane by ammonia, water, or a second borane molecule affects the B−H BDE only slightly, reducing it by a mere 1−5 kcal/mol relative to the free monomer. However, Table 1 demonstrates that coordinating ligands having π systems consistently and substantially diminish the BDE's. For instance, the B−H BDE of the carbon monoxide complex (BH_3·CO) was calculated at 78.6 kcal/mol, representing a decrease of 26.6 kcal/mol relative to free borane. Even larger effects are observed in the cases of HCN and HNC. Formaldehyde exerts the strongest influence of all, such that the BH_3·OCH_2 complex has a B−H BDE of 56 kcal/mol, representing a decrease of 49 kcal/mol compared to free borane! Larger ligands with π systems, such as acetone, acetonitrile, and pyridine, exhibit similar behavior.

Somewhat surprisingly, phosphine (PH_3) also leads to a significant reduction in the B−H BDE, despite the lack of a π system. The BDE in BH_3·PH_3 was calculated at 92.6 kcal/mol, 12.6 kcal/mol less than in free borane. BDE reductions

(10) Baldock, C.; Rafferty, J. B.; Sedelnikova, S. E.; Baker, P. J.; Stuitje, A. R.; Slabas, A. R.; Hawkes, T. R.; Rice, D. W. *Science* **1996**, *274*, 2107−2110.

(11) Curtiss, L. A.; Raghavachari, K.; Trucks, G. W.; Pople, J. A. *J. Chem. Phys.* **1991**, *94*, 7221−7230.

(12) Curtiss, L. A.; Carpenter, J. E.; Raghavachari, K.; Pople, J. A. *J. Chem. Phys.* **1992**, *96*, 9030−9034.

(13) Nyden, M. R.; Petersson, G. A. *J. Chem. Phys.* **1981**, *75*, 1843−1862.

(14) Petersson, G. A.; Al-Laham, M. A. *J. Chem. Phys.* **1991**, *94*, 6081−6090.

(15) Petersson, G. A.; Tensfeldt, T. G.; Montgomery, J. A., Jr. *J. Chem. Phys.* **1991**, *94*, 6091−6101.

(16) (a) Ochterski, J. W.; Petersson, G. A.; Montgomery, J. A., Jr. *J. Chem. Phys.* **1996**, *104*, 2598−2619. (b) Montgomery, J. A., Jr.; Ochterski, J. W.; Petersson, G. A. *J. Chem. Phys.* **1994**, *101*, 5900−5909.

(17) Ochterski, J. W.; Petersson, G. A.; Wiberg, K. B. *J. Am. Chem. Soc.* **1995**, *117*, 11299−11308.

Table 2. G-2 and CBS-4 Dissociation Enthalpies of Complexes (kcal/mol)

	0 K		298 K	
bond	G-2	CBS-4	G-2	CBS-4
BH_3-BH_3	36.3	36.8	38.2	38.8
BH_3-BH_2	41.2	42.1	43.0	43.9
H_3N-BH_3	26.1	26.8	27.8	28.6
H_3N-BH_2	29.1	29.7	30.8	31.5
H_2O-BH_3	10.3	8.6	11.6	10.1
H_2O-BH_2	11.1	9.7	12.4	11.1
H_3P-BH_3	20.5	23.0	21.8	24.3
H_3P-BH_2	33.1	36.6	34.5	38.0
$OC-BH_3$	21.5	21.9	22.8	23.3
$OC-BH_2$	48.1	50.5	49.6	52.0
$CO-BH_3$	0.9	−0.3	0.6	0.0
$CO-BH_2$	0.6	−3.0	1.7	−1.7
H_2CO-BH_3	12.4	10.9	13.5	12.1
H_2CO-BH_2	61.4	60.9	62.8	62.2
$HCN-BH_3$	15.4	15.1	16.6	16.3
$HCN-BH_2$	47.8	52.7	49.2	54.1
$HNC-BH_3$	29.6	30.5	30.9	31.9
$HNC-BH_2$	59.5	61.5	61.1	63.0
$(CH_3)_2O-BH_3$		16.9		18.0
$(CH_3)_2O-BH_2$		18.6		19.6
$H_3CCN-BH_3$		18.9		19.7
$H_3CCN-BH_2$		50.7		51.8
$(CH_3)_2S-BH_3$		23.2		24.1
$(CH_3)_2S-BH_2$		33.2		34.2
$(CH_3)_2CO-BH_3$		14.8		15.9
$(CH_3)_2CO-BH_2$		54.7		55.9
$(CH_3)_3N-BH_3$		36.5		38.1
$(CH_3)_3N-BH_2$		39.4		41.0
$(CH_3)_3P-BH_3$		39.1		40.0
$(CH_3)_3P-BH_2$		51.9		52.8
$(CH_3)_2SO-BH_3$		18.6		19.6
$(CH_3)_2SO-BH_2$		23.6		24.6
$THF-BH_3$		18.7		19.7
$THF-BH_2$		20.9		21.8
$pyridine-BH_3$		32.0		33.0
$pyridine-BH_2$		68.4		69.6

of a similar magnitude are observed in the cases of trimethylphosphine and dimethyl sulfide.

Unsuccessful attempts were made to study the complexes of borane with H_2S and HF. While the complex of borane with H_2S proved amenable to calculation, the corresponding radical spontaneously ejected a hydrogen atom from sulfur to yield BH_2SH and a hydrogen atom. Borane and HF did not form a stable complex at all.

Table 1 lists BDE's for the smallest systems at both the G-2 and CBS-4 levels of theory. Somewhat larger systems, such as the complexes of borane with pyridine, THF, and trimethylamine, are also included in the table, but energies are only reported at the more economical CBS-4 level of calculation. The analysis given below of why BDE's are so strongly affected in some cases, but not in others, focuses on the smaller systems for which the highest levels of calculation are accessible. However, the larger systems appear to be governed by the same principles, and so it is hoped that the understanding of coordination effects developed on the basis of the smaller systems will apply in a more general fashion to the larger systems as well.

Correlation of BDE's with Strength of Coordination. The heterolytic dissociation energies of the borane complexes are also of interest, and are reported in Table 2. The dissociation

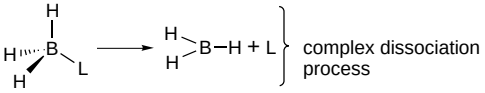

energies vary widely, from a low of 10 kcal/mol for $BH_3{\cdot}OH_2$ to a high of 36 kcal/mol for diborane. The complexes of borane with ammonia, carbon monoxide, trimethylamine, and formaldehyde have been calculated previously via high levels of ab initio theory, and the complexation energies obtained here agree well with those reported earlier.[18−23]

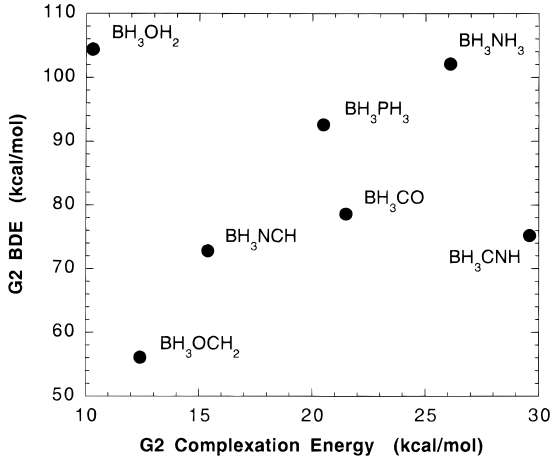

Figure 1. Plot of calculated homolytic B−H bond dissociation enthalpy versus heterolytic dissociation enthalpy of the complex. The enthalpies were calculated via the G2 procedure and correspond to absolute zero. The dissociation enthalpies are for the closed-shell complexes. Correlation coefficient = 0.013.

The species providing the most tightly bound complexes are not the ones exerting the strongest influence on B−H BDE's. As a case in point, the strongest complexation (diborane; 36 kcal/mol) occurs in a case where the BDE is minimally affected (5 kcal/mol), whereas the largest effect on BDE (49 kcal/mol) derives from a ligand that associates only weakly (formaldehyde; 12 kcal/mol). This lack of correlation is demonstrated more generally in Figure 1, which depicts the relationship between B−H BDE and complex dissociation energy. The data points do not conform to any pattern whatsoever, and in fact the correlation coefficient is calculated at 0.013! Although perhaps initially surprising, the lack of a simple relationship is easily understood. A large decrease in the B−H BDE relative to free borane can only occur if the Lewis base binds to BH_2 much more strongly than to BH_3, and so only this *difference* in binding energies can affect the BDE.

Geometry of Complexes. The extent of geometric perturbation occurring upon hydrogen atom abstraction correlates with the magnitude of the B−H BDE. Figures 2 and 3 show the structures of some of the borane complexes and their associated radicals, calculated at the MP2/6-31G* level of theory, which is known to reproduce molecular geometries reliably and accurately.[24] Table 3 provides numerical values for some key bond distances and angles. The B−X bond lengths in $BH_3{\cdot}$

(18) McKee, M. L. *J. Phys. Chem.* **1992**, *96*, 5380−5385.
(19) Sakai, S. *J. Phys. Chem.* **1995**, *99*, 5883−5888.
(20) Røeggen, I. *Chem. Phys.* **1992**, *162*, 271−284 and references therein.
(21) Redmon, L. T.; Purvis, G. D., III; Bartlett, R. J. *J. Am. Chem. Soc.* **1979**, *101*, 2856−2862.
(22) Umeyama, H.; Morokuma, K. *J. Am. Chem. Soc.* **1976**, *98*, 7208−7220.
(23) LePage, T. J.; Wiberg, K. B. *J. Am. Chem. Soc.* **1988**, *110*, 6642−6650.

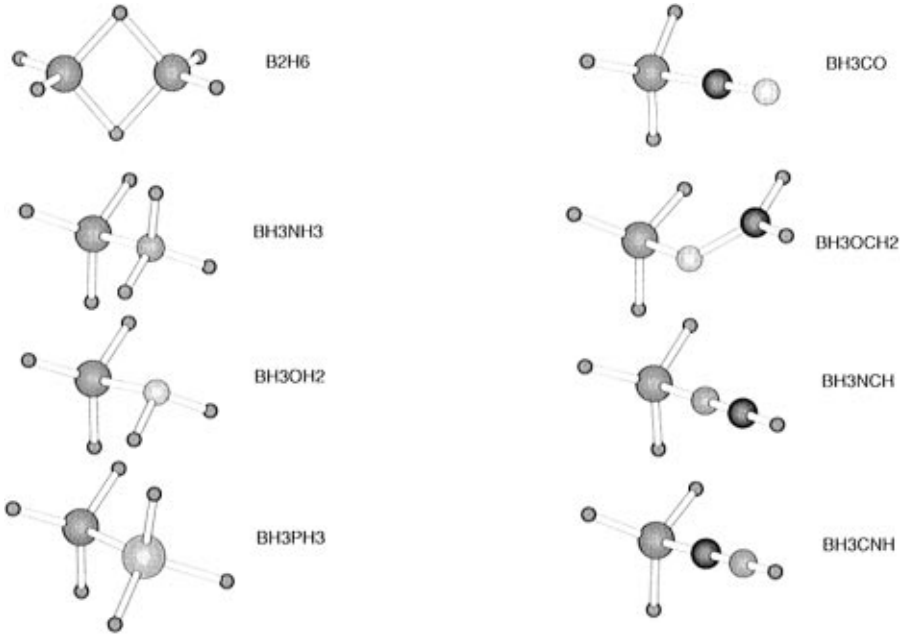

Figure 2. Geometries of the closed-shell borane complexes calculated at the MP2/6-31G* level of theory.

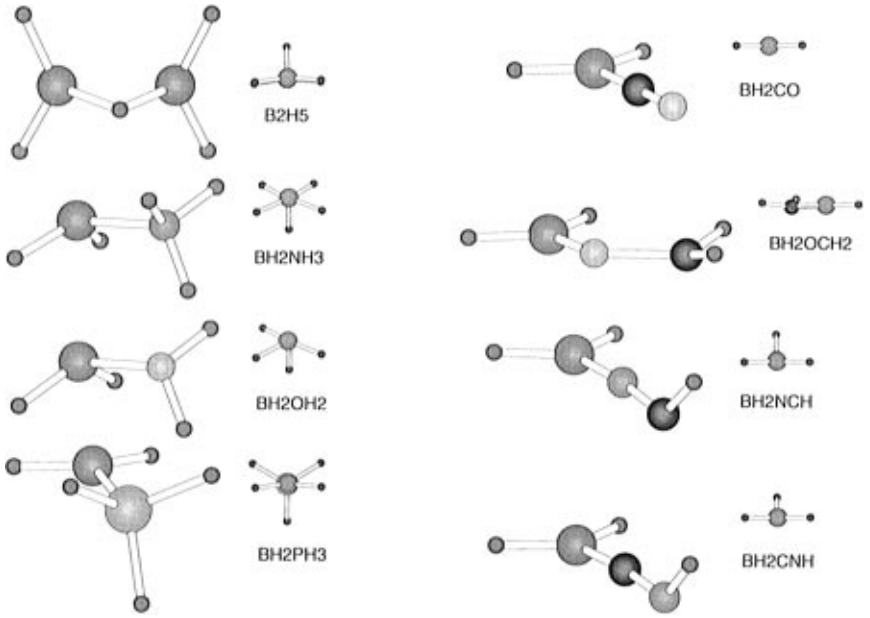

Figure 3. Geometries of the open-shell borane complexes calculated at the MP2/6-31G* level of theory.

NH_3 and $BH_3{\cdot}OH_2$ change very little as the result of abstracting a boron-bound hydrogen atom, while those in $BH_3{\cdot}PH_3$, $BH_3{\cdot}CO$, $BH_3{\cdot}OCH_2$, $BH_3{\cdot}NCH$, and $BH_3{\cdot}CNH$ decrease quite substantially and suggest strong stabilization of the corresponding radicals. This relationship is shown in Figure 4, where the B−H BDE is plotted against the corresponding percentage change in the B−X bond length. While certainly not perfect, the correlation is nonetheless significant, and yields a correlation coefficient of 0.79. Furthermore, the imperfection in correlation arises predominantly from two outlying points, for $BH_3{\cdot}CO$ and $BH_3{\cdot}CNH$, and if these are excluded the correlation coefficient for the remaining points increases to 0.99. Apparently, B−C bonds respond more strongly to changes in electronic structure than do other types of B−X bonds.

The BDE's also correlate with bond angles and the degree of pyramidalization at boron and other associated atoms. In the complexes with the least perturbed BDE's (H_2O, NH_3, diborane), boron is pyramidalized in the radical and has HBH bond angles very similar to those in the closed-shell complexes. In the complexes with substantially weakened BDE's, however, the boron atom is consistently planarized. Such an arrangement forces the unpaired electron into a p-orbital capable of interacting with π^* orbitals on the associating Lewis base or, in the case of phosphine, either empty d-orbitals or P−H σ^* antibonding orbitals. The geometric perturbations thus suggest that the unpaired electron is delocalized onto the associating Lewis base.

Changes of geometry at heteroatoms other than boron also provide some useful clues about electronic structure. The molecules HCN and HNC preserve their linearity on complexation with BH_3, but become strongly bent upon hydrogen atom abstraction to form $BH_2{\cdot}NCH$ and $BH_2{\cdot}CNH$. Formaldehyde also preserves its basic molecular shape in its complex with BH_3, but becomes quite strongly pyramidalized in $BH_2{\cdot}OCH_2$.

(24) Hehre, W. J.; Radom, L.; Schleyer, P. v. R.; Pople, J. A. *Ab Initio Molecular Orbital Theory*; Wiley: New York, 1986.

Table 3. Geometric Parameters, MP2/6-31G*

H_3B-BH_3	*r*(B−B):	1.7527				
H_3B-BH_2	*r*(B−B):	1.7639				
change	*r*(B−B):	+1.01%				
H_3N-BH_3	*r*(B−N):	1.6627				
H_3N-BH_2	*r*(B−N):	1.6400				
change	*r*(B−N):	−1.36%				
H_2O-BH_3	*r*(B−O):	1.7291				
H_2O-BH_2	*r*(B−O):	1.7023				
change	*r*(B−O):	−1.55%				
H_3P-BH_3	*r*(B−P):	1.9435				
H_3P-BH_2	*r*(B−P):	1.8606				
change	*r*(B−P):	−4.27%				
$OC-BH_3$	*r*(B−C):	1.5468	*r*(C−O):	1.1481		
$OC-BH_2$	*r*(B−C):	1.4817	*r*(C−O):	1.1661		
change	*r*(B−C):	−4.21%	*r*(C−O):	+1.57%		
H_2CO-BH_3	*r*(B−O):	1.6861	*r*(C−O):	1.2331	*t*(HCOH):	180.0°
H_2CO-BH_2	*r*(B−O):	1.3613	*r*(C−O):	1.3739	*t*(HCOH):	155.0°
change	*r*(B−O):	−19.3%	*r*(C−O):	+11.4%	*t*(HCOH):	−25.0°
$HCN-BH_3$	*r*(B−N):	1.5875	*r*(C−N):	1.1648	*a*(HCN):	180.0°
$HCN-BH_2$	*r*(B−N):	1.3998	*r*(C−N):	1.1932	*a*(HCN):	131.1°
change	*r*(B−N):	−11.8%	*r*(C−N):	+2.44%	*a*(HCN):	−48.9°
$HNC-BH_3$	*r*(B−C):	1.5600	*r*(C−N):	1.1718	*a*(HNC):	180.0°
$HNC-BH_2$	*r*(B−C):	1.4763	*r*(C−N):	1.2088	*a*(HNC):	132.2°
change	*r*(B−C):	−5.37%	*r*(C−N):	+3.16%	*a*(HNC):	−47.8°

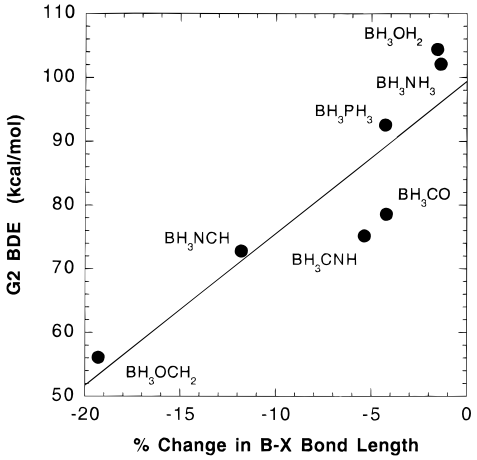

Figure 4. Plot of calculated B−H bond dissociation enthalpy versus percentage change in B−X bond length occurring upon hydrogen abstraction. Correlation coefficient = 0.79.

Both these observations are consistent with the delocalization of radical character away from boron and into the π systems of HCN, HNC, and H_2CO.

Correlation of BDE's with Spin Density Delocalization. The geometric changes that accompany bond dissociation offer tantalizing clues as to the nature of stabilization in the complexes that exhibit markedly decreased B−H BDE's. However, one of the advantages of ab initio MO methodology is that one obtains not only molecular structures and energies but also wave functions. The wave function in turn provides the spin density, defined as the difference in probability density between electrons with α and β spin. The spin density thus describes the "location" of the unpaired electron in a radical.[25]

Figure 5 depicts the calculated spin density distributions for a series of complexes of borane radical. The surfaces drawn represent iso-spin density contours, i.e., they depict the surfaces at which the spin density is ±0.002 electrons per cubic bohr. The solid lines represent positive spin density (excess α spin) while the dashed lines represent negative spin density (excess β spin). Wiberg has shown that QCISD wave functions with large basis sets are often required to obtain accurate spin densities, and so the QCISD/6-311+G**(6D)//MP2/6-31G* level of theory was chosen for this purpose.[26]

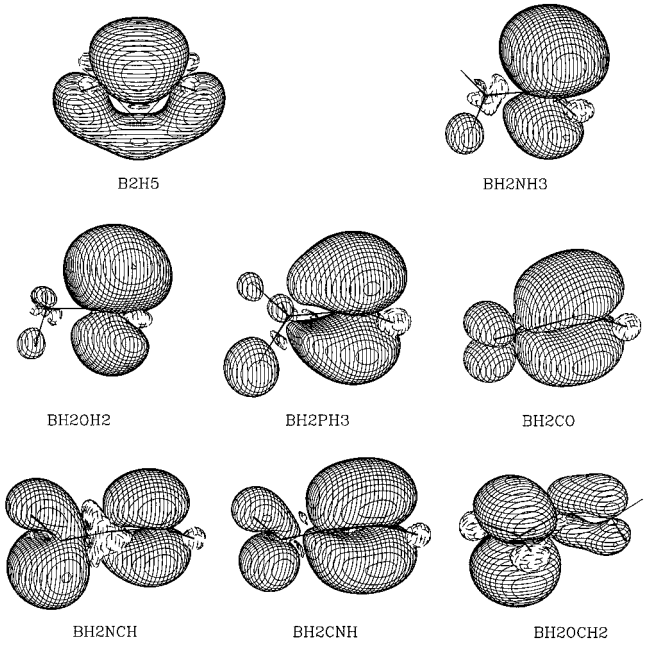

Figure 5. QCISD/6-311+G**(6D)//MP2/6-31G* calculated spin density distributions for radicals obtained by hydrogen atom abstraction from 4-coordinate borane complexes. The surfaces depicted represent the $\pm 2.0 \times 10^{-3}$ electron/bohr^3 contours. The solid lines represent positive spin density and the dashed lines represent negative spin density. The molecules are all oriented with the BH_2 group on the right-hand side.

Even a cursory examination reveals that the delocalization of spin density correlates with BDE. When NH_3 or H_2O is the ligand, and the B−H BDE is barely perturbed, the α spin is almost entirely restricted to the vicinity of the boron atom. In

(25) Fessenden, R. W.; Schuler, R. H. *J. Chem. Phys.* **1963**, *39*, 2147−2195.

(26) Wiberg, K. B.; Cheeseman, J. R.; Ochterski, J. W.; Frisch, M. J. *J. Am. Chem. Soc.* **1995**, *117*, 6535−6543

Table 4. Spin Density Populations of Radicals, QCISD/6-311+G**(6D)

radical	fragment/atom	AIM	NPA
BH_3-BH_2	BH_2	0.500	0.500
H_3N-BH_2	BH_2	0.898	0.978
	NH_3	0.102	0.022
H_2O-BH_2	BH_2	0.934	0.989
	H_2O	0.066	0.011
H_3P-BH_2	BH_2	0.658	0.805
	PH_3	0.342	0.195
$OC-BH_2$	BH_2	0.351	0.506
	C	0.448	0.284
	O	0.202	0.210
H_2CO-BH_2	BH_2	0.044	0.060
	O	0.101	0.030
	CH_2	0.855	0.910
$HCN-BH_2$	BH_2	0.158	0.233
	N	0.138	0.009
	HC	0.704	0.759
$HNC-BH_2$	BH_2	0.282	0.410
	C	0.470	0.341
	HN	0.248	0.249

the remaining cases, where the B−H BDE is at least moderately affected, the α spin is clearly distributed over other parts of the molecule as well.

Various schemes exist for calculating atomic electron populations from molecular wave functions.[27] Although the wide disparity in numerical results sometimes obtained from the different procedures can lead to some difficulty in drawing conclusions, it has been documented that *differences* in atomic populations, when assessed consistently by using a single definition, are generally meaningful.[27] Many of the procedures that yield atomic charges can equally well be used to obtain atomic spin density populations. In an attempt to quantify the extent of delocalization, spin density populations have been computed by using both the Atoms in Molecules (AIM) approach of Bader[28−30] and the Natural Population Analysis (NPA) of Weinhold,[31,32] and the results are given in Table 4. The former procedure is based on a division of physical space into atomic regions according to topological principles, while the latter represents a modification of the Mulliken definition that largely removes the problem of basis set dependence.

The spin density data in Table 4 clearly demonstrate a relationship between the B−H BDE and the extent to which radical character is transferred away from boron. The relationship is illustrated graphically in Figure 6, where the BDE is plotted against the fraction of α spin density found outside the BH_2 fragment.[33] The excellent correlation ($R^2 = 0.96$) suggests that delocalization of the unpaired electron on boron and the corresponding stabilization of the radical is the primary cause of the reduced B−H BDE's. Whether this stabilization results primarily from the delocalization per se or rather from transfer

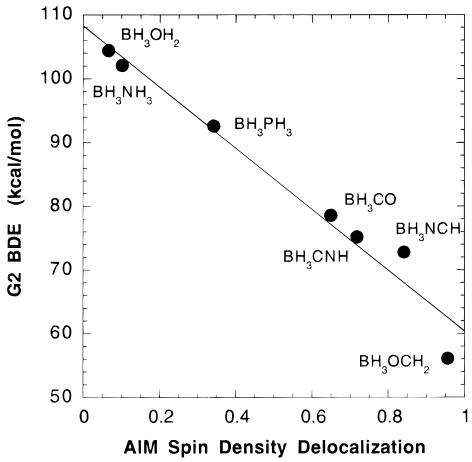

Figure 6. Plot of calculated B−H bond dissociation enthalpy versus spin density delocalization calculated via the AIM procedure. The enthalpies were calculated via the G2 procedure and correspond to absolute zero. The spin density populations were computed by using QCISD/6-311+G**(6D) wave functions at the MP2/6-31G* optimized geometries. The spin density delocalization is defined here as the total quantity of α spin density on atoms other than the BH_2 fragment. Correlation coefficient = 0.96.

of the unpaired electron from boron to some other atom better able to accommodate radical character is not immediately evident. However, the fact that the most stable radicals (lowest B−H BDE's) are the ones in which most of the spin density resides on carbon suggests that the latter interpretation has some validity.

Detailed Interpretation of Spin Densities for Individual Molecules. Detailed examination of the spin densites in Figure 5 shows that the distribution of radical character is in accord with qualitative molecular orbital and resonance arguments. In the case of $BH_2 \cdot PH_3$, which has a moderately perturbed B−H BDE, the majority of spin density resides on boron, but a significant quantity also exists on phosphorus and on the hydrogen atom lying in the plane of symmetry. The transfer of spin density can be attributed to interaction of the half-filled p orbital on boron with either the d or the σ_{PH}* orbitals on phosphorus. The former interaction is depicted below, using both molecular orbital and resonance formalism.

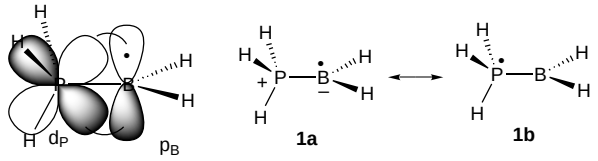

However, the interpretation invoking σ_{PH}* orbitals is perhaps preferred, as d-orbitals have been shown previously to play only a minor role in phosphorus and sulfur compounds.[34] Furthermore, as phosphorus is more electropositive than hydrogen, the σ_{PH}* orbitals are strongly polarized toward phosphorus, and overlap with boron should be favorable. The region of α spin density appearing on the "anti" hydrogen on phosphorus also implicates the σ_{PH}* orbital, as does the 0.02 Å greater length of the "anti" P−H bond relative to the others. The interaction with the σ_{PH}* orbital is shown below schematically.

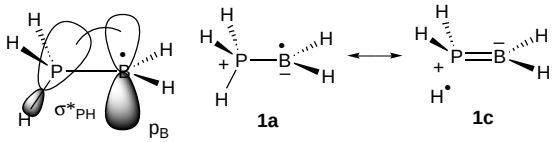

(27) Wiberg, K. B.; Rablen, P. R. *J. Comput. Chem.* **1993**, *14*, 1504−1518.

(28) Bader, R. F. W. *Atoms in Molecules*; Clarendon Press: Oxford, UK, 1990.

(29) Bader, R. F. W. *Chem. Rev.* **1991**, *91*, 893−928.

(30) Bader, R. F. W. *Acc. Chem. Res.* **1985**, *18*, 9−15.

(31) Reed, A. E.; Weinstock, R. B.; Weinhold, F. *J. Chem. Phys.* **1985**, *83*, 735−746.

(32) Reed, A. E.; Curtiss, L. A.; Weinhold, F. A. *Chem. Rev.* **1988**, *88*, 899−926.

(33) Figure 6 represents the spin densities derived from the AIM definition. However, the results obtained by using the NPA spin density populations are essentially identical, as the NPA and AIM charges are linearly related with a correlation coefficient of 0.98. Details are provided in the Supporting Information.

The BH_2·CO complex also exhibits delocalization of spin density. The node appearing between carbon and oxygen suggests that this delocalization results from interaction of the singly occupied boron p-orbital with the π_{CO}* orbital, as shown below.[35]

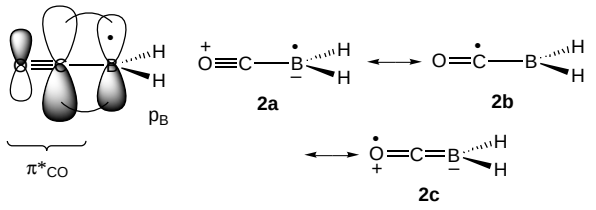

The greatest concentration of spin density is found on boron (43%) and carbon (37%), with a lesser amount on oxygen (20%), in agreement with the lesser importance of structure **2c** (which is electron deficient at oxygen) relative to **2a** and **2b**.[36]

The complexes of BH_2 with HCN and HNC exhibit similar behavior. Here, delocalization requires an allene-like resonance structure, suggesting that the terminal hydrogen needs to be in a plane perpendicular to the BH_2 group, in accord with the observed molecular geometry. The spin density distributions mirror quite closely those predicted by resonance arguments. In the case of BH_2·NCH, spin density is almost exclusively located on carbon (73%), with only a modest amount at boron (20%) and a very small amount at nitrogen (7%). This distribution is in accord with the three most reasonable resonance structures, which place radical character on carbon and boron but not nitrogen.[37] The only way to place spin density at nitrogen would be through a highly unfavorable resonance structure that is electron deficient at nitrogen and anionic at carbon. BH_2·CNH can be described in a somewhat similar fashion, except that the most reasonable structures place spin density at all three centers, boron, carbon, and nitrogen.[38]

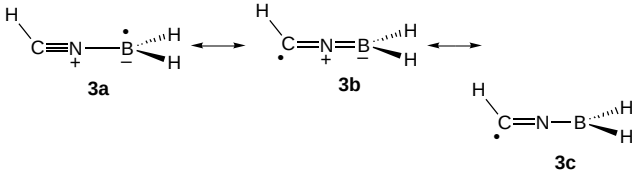

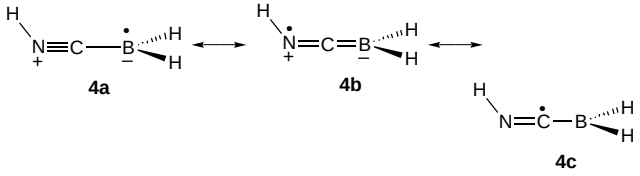

Again, the spin density distribution in Figure 5 corresponds closely to this picture, with delocalization of α spin to both carbon (41%) and nitrogen (25%) clearly evident.

Formaldehyde exerts the strongest influence on BDE of any of the small Lewis bases studied here. The spin density distribution for BH_2·OCH_2 shows that the majority of radical character is on carbon (86%), with only a small amount on boron (4%) or oxygen (10%). The shape of the spin density distribution around the carbonyl closely resembles a π* orbital, which would be expected to have a larger coefficient on carbon than on oxygen. Resonance structures once again correctly rationalize the observed distribution of spin density.

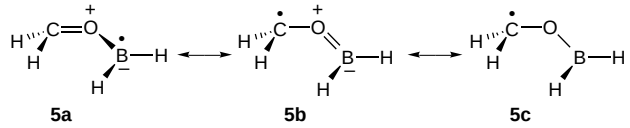

Alternative Bond Dissociation Pathways. For some of the borane radicals studied here, the reverse of the bond dissociation process can take place at an atom other than boron, as shown in Scheme 1. For instance, the BH_2·OCH_2 radical can be derived by hydrogen atom abstraction from either BH_3·OCH_2 *or* BH_2OCH_3. Table 1 contains the BDE's for these alternative dissociation routes. In the case of formaldehyde as ligand, the results suggest an alternative way of viewing the B−H BDE. In isolation, B−H bonds are slightly stronger than typical C−H bonds. The BDE for a C−H bond in BH_2OCH_3 (Scheme 1) is calculated at 98.8 kcal/mol, representing a fairly typical value. The ordinary nature of this BDE suggests that the resulting radical species is also quite ordinary. Why, then, is the B−H BDE of BH_3·OCH_2 so extraordinary? One can attribute the low BDE to instability of the spin paired species, BH_3·OCH_2, as easily as to stability of the radical. From this perspective, the low B−H BDE of BH_3·OCH_2 results from the fact that whereas BH_3·OCH_2 is merely a donor−acceptor complex of borane and formaldehyde, with a relatively weak B-O bond, BH_2·OCH_2 represents a radical derived from a true, fully

(34) Kutzelnigg, W. *Angew. Chem., Int. Ed. Engl.* **1984**, *23*, 272−295.

(35) The resonance structures below might also reasonably be considered:

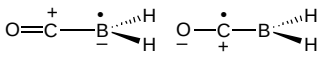

However, inclusion of these structures simply emphasizes the polarization of the carbonyl bond, which is already present in the closed-shell complex BH_3CO. Consequently, these structures do not represent any delocalization not already present before hydrogen atom abstraction takes place, and so they are ignored in this analysis.

(36) The atomic spin density populations reported in this portion of the text are the average of the AIM and NPA determinations, which are described in detail in the next section.

(37) The criteria used here for "good" resonance structures are as follows: (a) more bonds are preferred to fewer, unless reducing the number of bonds removes separation of charge; (b) fewer than seven electrons around an atom is disfavored; (c) if an atom is to be both a radical and a cationic center, it should not be on an electronegative element such as nitrogen or oxygen. In the case of BH_2NCH shown here, structures **3a** and **3b** have the maximum number of bonds between carbon, nitrogen, and boron, and so are favored. Structure **3c** has one fewer bond, but there is no charge separation, so it also is favored. Structure **3d** is disfavored both because the number of bonds is reduced (as in structure **3c**, but without a reduction in the degree of charge separation) and also because the electronegative nitrogen is electron deficient.

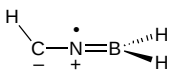

The bent geometry at carbon (requiring sp^2 hybridization) implies that structure **3a** (which strictly speaking requires sp hybridization at C) is not rigorously correct. The alternative structure **3e** below corrects this problem, and can be thought of as a substitute for **3a**. The replacement of **3a** with **3e** does not affect predictions of where spin density will be located, and merely represents polarization of the C-N π electrons, and so this issue is not pursued further here.

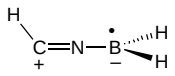

(38) The bent geometry at nitrogen (requiring sp^2 hybridization) implies that structure **4a** (which strictly speaking requires sp hybridization at N) is not rigorously correct. The alternative structure **4d** below corrects this problem, and can be thought of as a substitute for **4a**, just as **3f** serves as a substitute for **3a** in BH_2NCH. The replacement of **4a** with **4d** does not affect predictions of where spin density will be located, and merely represents polarization of the C-N π electrons, and so this issue is not pursued further here.

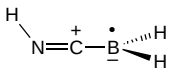

Table 5. Sharing Indices, QCISD/6-311+G**(6D)

species	B−X	B−H	X−H	X_1-X_2	X_2-H
BH_3-BH_3	0.054	0.511 × 4/0.299 × 2			
BH_3-BH_2	0.181	0.567 × 4/0.459 × 1			
H_3N-BH_3	0.289	0.469	0.721		
H_3N-BH_2	0.434	0.639	0.717 (av)		
H_2O-BH_3	0.212	0.477 (av)	0.560		
H_2O-BH_2	0.341	0.644	0.554 (av)		
H_3P-BH_3	0.376	0.496	0.680		
H_3P-BH_2	0.663	0.647	0.679 (av)		
$OC-BH_3$	0.377	0.476		1.358	
$OC-BH_2$	0.605	0.564		1.404	
H_2CO-BH_3	0.219	0.473 (av)		1.173	0.776 (av)
H_2CO-BH_2	0.466	0.486 (av)		0.888	0.837 (av)
$HCN-BH_3$	0.279	0.469		1.820	0.787
$HCN-BH_2$	0.510	0.515		1.547	0.798
$HNC-BH_3$	0.375	0.471		1.510	0.615
$HNC-BH_2$	0.588	0.542		1.556	0.677

Scheme 1. Alternative Bond Dissociation Pathways

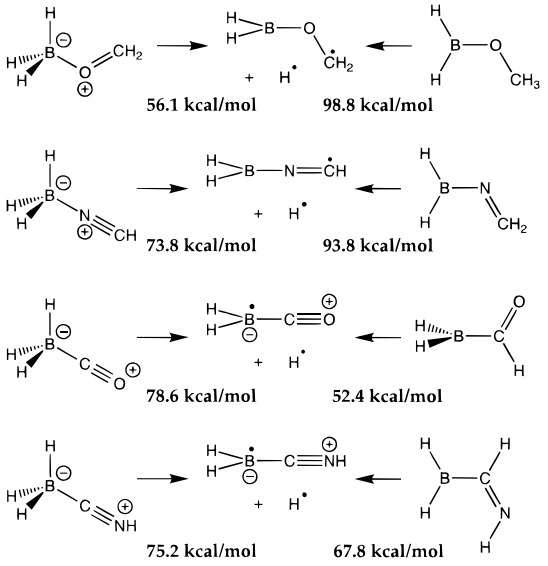

covalent molecule, BH_2OCH_3. In other words, the true parent species to $BH_2{\cdot}OCH_2$ is not $BH_3{\cdot}OCH_2$ but rather BH_2OCH_3, for which the bond dissociation process requires a very ordinary amount of energy.

Similar logic can be applied to the complex of borane with HCN, as shown in Scheme 1. Here, the BDE for the alternative process (C−H cleavage from BH_2NCH_2) is 93.8 kcal/mol, again a fairly unremarkable C−H BDE, and substantially larger than the B−H BDE for the corresponding species on the left. The possibility exists for similar analyses in the cases of $BH_2{\cdot}CNH$ and $BH_2{\cdot}CO$ (Scheme 1), but the alternative spin-paired species are less stable than the corresponding donor−acceptor complexes, and so the corresponding BDE's are not higher (more "ordinary").

Correlation of BDE's and Strength of Association with a Measure of Covalent Bond Order. Some of the resonance structures drawn earlier, such as **2c**, suggest that the delocalization of spin density away from boron should be correlated with increased bonding between boron and the Lewis base coordinated to it. Fulton has defined a sharing index,[39,40] closely related to Cioslowski's covalent bond order,[41] that describes the extent to which electrons are irreducibly shared between atoms in a molecule. Sharing indices have been calculated at the QCISD/6-311++G**(6D)//MP2/6-31G* level in order to quantify covalent interaction and explore its role in stabilization, and they are reported in Table 5. A value of 1 corresponds to a fully covalent single bond composed of a pair of electrons.

Partial double bond character in the B−C bond of a BH_2 radical complex, as in resonance structure **2c**, might be expected to result in an increased sharing index compared to the corresponding spin-paired borane complex, for which no resonance structure containing a B−C double bond can be drawn. However, comparison of the B−H BDE's with the corresponding changes in the B−X sharing index shows little or no relationship between the two ($R^2 = 0.53$). Apparently, stabilization of the radical is not correlated with the extent of covalency, at least as defined by Fulton's sharing index. Interestingly, further examination reveals that the association enthalpies of the closed-shell complexes *do* correlate with the sharing index, as shown in Figure 7. However, such correlation is absent for the radicals, and thus also for the BDE's.

Stabilization probably has more to do with spin polarization and the transfer of spin density to atoms that stabilize radical character more efficiently than boron. For instance, the primary locus of spin density is carbon for all of the four substituents CO, HCN, HNC, and H_2CO that lead to the most highly stabilized radicals. This trend might reflect the particular stability associated with carbon-centered radicals. The case of PH_3 demonstrates that there is some benefit in transferring spin density from boron to phosphorus as well. These observations are in agreement with the findings of Wiberg, who observed in a series of heterosubstituted allyl radicals that the spin density accumulated preferentially on the least electronegative atom.[42]

Charge Density Redistribution Occurring as a Result of Association. Crystallographers have long used deformation density plots to depict the differences in electron density for a molecule relative to its constituent atoms.[43,44] A similar approach can be used to compare the calculated charge density distributions for related molecules. For instance, charge density difference plots[45] have been used to illustrate how such factors as inclusion of electron correlation or of particular basis

(39) Fulton, R. L. *J. Phys. Chem.* **1993**, *97*, 7516−7529.
(40) Fulton, R. L.; Mixon, S. T. *J. Phys. Chem.* **1993**, *97*, 7530−7534.
(41) Cioslowski, J.; Mixon, S. T. *J. Am. Chem. Soc.* **1991**, *113*, 4142−4145.
(42) Wiberg, K. B.; Cheeseman, J. R.; Ochterski, J. W.; Frisch, M. J. *J. Am. Chem. Soc.* **1995**, *117*, 6535−6543.
(43) Coppens, P. In *Electron Distributions in the Chemical Bond*; Hall, M. B., Ed.; Plenum Press: New York, 1982; pp 61−92.
(44) Dunitz, J. D. *X-Ray Analysis and the Structure of Organic Molecules*; Cornell University Press: Ithaca, NY, 1979.

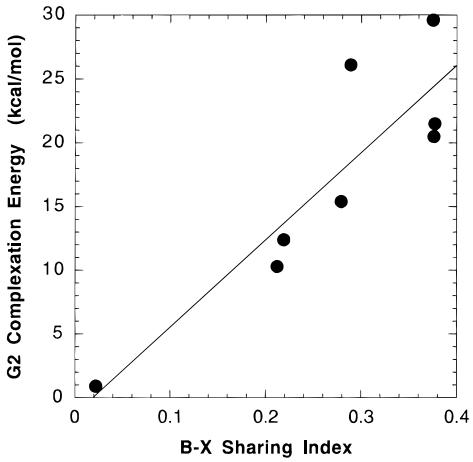

Figure 7. Plot of calculated complexation enthalpy of borane with various Lewis bases versus the calculated sharing index for the B−X bond. The enthalpies were calculated via the G2 procedure and correspond to absolute zero. The sharing indices were computed by using QCISD/6-311+G**(6D) wave functions at the MP2/6-31G* optimized geometries. Best fit line: BDE = 68.4SI − 1.29; correlation coefficient = 0.79.

functions affect the molecular charge distribution,[46] to illustrate the reorganization of charge upon electronic excitation,[47] to depict the effect of hydrogen bonding,[48] and to visualize and quantify the intramolecular charge transfer that occurs during bond rotation in conjugated systems.[49]

The same approach is used here to compute the charge density reorganization that occurs upon complexation of either BH_3 or BH_2 to a Lewis base. The charge density is first computed at the QCISD/6-311+G**(6D)//MP2/6-31G* level of theory for the entire complex. From this total density, the independent charge density distributions of the individual molecules comprising the complex are then subtracted. For instance, for $BH_3{\cdot}NH_3$, the distributions for BH_3 and NH_3 are subtracted from that for $BH_3{\cdot}NH_3$.[50] Difference densities for association of closed-shell borane complexes are shown in Figure 8, and those for the corresponding radicals are shown in Figure 9.

The extent of electronic reorganization occurring upon complexation was quantified by direct integration of the difference density distributions appearing in Figures 8 and 9.[51] The total charge reorganization computed in this manner showed a limited correlation ($R^2 = 0.71$) with the enthalpy of association, such that a greater extent of charge redistribution corresponded to a greater change in enthalpy. This behavior is consistent with what occurs during bond rotation in conjugated systems, where the quantity of intramolecular charge transfer is only weakly correlated with the magnitude of the rotational barrier.[49]

(45) Wiberg, K. B.; Hadad, C. M.; Breneman, C. M.; Laidig, K. E.; Murcko, M. A.; LePage, T. J. *Science* **1991**, *252*, 1266−1272.

(46) Wiberg, K. B.; Castejon, H. *J. Am. Chem. Soc.* **1994**, *116*, 10489−10497.

(47) Walters, V. A.; Hadad, C. M.; Thiel, Y.; Colson, S. D.; Wiberg, K. B.; Johnson, P. M.; Foresman, J. B. *J. Am. Chem. Soc.* **1991**, *113*, 4782−4791. Wiberg, K. B.; Hadad, C. M.; Foresman, J. B.; Chupka, W. A. *J. Phys. Chem.* **1992**, *96*, 10756−10768. Hadad, C. M.; Foresman, J. B.; Wiberg, K. B. *J. Phys. Chem.* **1993**, *97*, 4293−4312.

(48) Gao, J.; Xia, X. *Science* **1992**, *258*, 631−635.

(49) Wiberg, K. B.; Rablen, P. R. *J. Am. Chem. Soc.* **1995**, *117*, 2201−2209. Wiberg, K. B.; Rablen, P. R. *J. Am. Chem. Soc.* **1993**, *115*, 9234−9242.

(50) Subtractions were performed while holding the geometries of the separate fragments constant. Control calculations, described in the Supporting Information, showed that little error was introduced by the required geometric constraints.

(51) To be more precise, the absolute values of the difference density distributions were integrated, since integration of the difference density *including* sign would necessarily yield a value of zero.

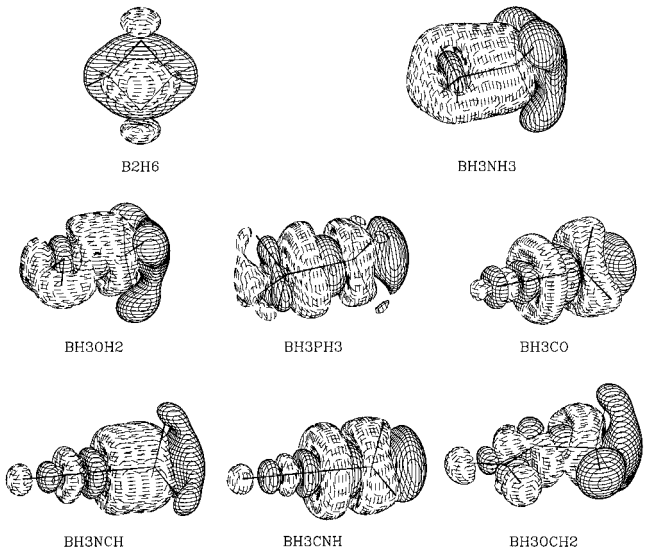

Figure 8. QCISD/6-311+G**(6D)//MP2/6-31G* calculated difference densities for closed-shell borane complexes. The surfaces shown represent the $\pm 2.0 \times 10^{-3}$ electron/bohr^3 contours. The solid lines represent positive electron density and the dashed lines represent negative electron density. The difference density is defined here as the electron density for the complex (BH_3−X) minus the electron density distributions for the isolated components (BH_3 and X).

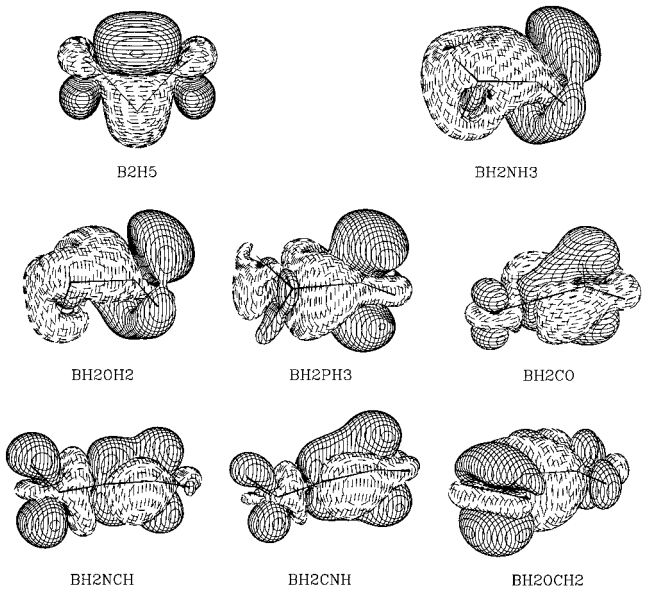

Figure 9. QCISD/6-311+G**(6D)//MP2/6-31G* calculated difference densities for open-shell borane complexes obtained by hydrogen atom abstraction from the corresponding closed-shell complexes. The surfaces shown represent the $\pm 2.0 \times 10^{-3}$ electron/bohr^3 contours. The solid lines represent positive electron density and the dashed lines represent negative electron density. The difference density is defined here as the electron density for the complex (BH_2−X) minus the electron density distributions for the isolated components (BH_2 and X).

Larger Systems. Table 1 includes B−H BDE's calculated at the CBS-4 level of theory for several complexes of borane with Lewis bases somewhat larger than the small systems discussed thus far. These species, such as pyridine, THF, trimethylamine, trimethylphosphine, dimethyl ether, and dimethyl sulfide, represent examples that might interest experimentalists, as they correspond more closely to compounds frequently used in the laboratory than do the "minimalist" model systems used in the earlier analysis. Qualitatively, however, the BDE's follow the same patterns observed earlier, and the foregoing analysis provides the information necessary to understand the additional data.

Those ligands lacking a π system generally have only a small effect on the B−H BDE. Thus, for instance, trimethylamine, dimethyl ether, and THF yield B−H BDE's that differ by no more than 1.1 kcal/mol from those in the complexes with ammonia and water. The case of phosphine demonstrated earlier that second-row elements have a somewhat stronger effect on the B−H BDE, and this observation extends to the larger systems as well. The effect of trimethylphosphine (12.7 kcal/mol reduction in B−H DBE relative to free borane) is essentially identical with that of phosphine (13.5 kcal/mol), and that of dimethyl sulfide (10.0 kcal/mol) is comparable as well. The latter case suggests that the BDE reduction in the phosphine complexes is a general characteristic of second-row elements, and not particular to phosphorus. DMSO has a modest effect on the BDE, reducing it by 5.0 kcal/mol relative to borane. Apparently DMSO does not act like a molecule with a true π system, and the more distant location of the sulfur relative to boron (one atom removed) seems to attenuate its influence.

The larger bases with π systems have more substantial effects on the BDE's that also parallel the patterns observed with the smaller molecules. Acetonitrile and acetone behave in a manner similar to HCN and formaldehyde, respectively, although in each case the effects are attenuated by 5−10 kcal/mol relative to the smaller ligands. It is interesting that the methylated derivatives actually have a *weaker* effect on the B−H BDE's than do the smaller systems, given that methyl substituents generally stabilize radical character. Finally, pyridine has an effect very similar in magnitude to that of acetone and acetonitrile.

Summary

Ab initio molecular orbital calculations at the G-2 and CBS-4 levels of theory have shown that B−H bonds of four-coordinate boron are generally weaker than those of three-coordinate boron. The effect varies from very small, in the case of NH_3 or H_2O as the coordinating ligand, to very large, in the cases of HCN, HNC, formaldehyde, or CO. Compounds of second-row elements such as phosphorus and sulfur have an intermediate effect. The magnitude of the decrease in the BDE is not correlated with the strength of coordination. However, it is closely correlated with the degree to which spin density in the radical is delocalized away from boron and onto the atoms of the associated ligand. The strongest perturbations occur in those cases where the presence of a π-system facilitates delocalization of the spin density, and there appears to be a preference for delocalizing the spin density selectively onto carbon atoms. Formaldehyde represents the most extreme case of such a coordinating ligand, with over 90% of the spin density located on carbon, and the B−H BDE reduced from 104 kcal/mol (free borane) to 56 kcal/mol.

Acetone, acetonitrile, trimethylamine, tetrahydrofuran, dimethyl sulfoxide, dimethyl ether, trimethylphosphine, dimethyl sulfide, and pyridine were also examined as coordinating ligands, although in somewhat lesser computational detail. The effects on B−H BDE's are in accord with the trends observed for the smaller species. Pronounced reductions occur only in the presence of a second-row atom (sulfur or phosphorus) or a π-system capable of delocalizing the unpaired electron.

Calculations

All ab initio calculations were performed with the Gaussian 94 package.[52] All structures for which G-2 energies[11] are listed in Table A (Supporting Information) were verified as minima by calculation of the vibrational frequencies at the HF/6-31G* level of theory in the course of the G-2 procedure, i.e., no imaginary frequencies were found. The CBS-4 method developed recently by Ochterski and Petersson[16,17] is now also implemented directly in Gaussian 94. All structures for which CBS-4 energies are listed in Table A were verified as minima by calculation of the vibrational frequencies at the HF/3-21G* level in the course of the CBS-4 procedure.

The G-2 and CBS-4 methods by themselves give enthalpies at absolute zero. The thermodynamic corrections necessary to convert these to enthalpies at 298 K were carried out by treating the translational, rotational, and vibrational components in the standard manner,[53] using the program THERMO written at Yale University.[54] The HF/3-21G* frequencies scaled by 0.9167 were used to make corrections for the CBS-4 energies, while HF/6-31G* frequencies scaled by 0.8934 were used to make corrections to the G-2 energies. These are the same levels of calculation and scaling factors used for the zero point vibrational energies. All vibrational modes were treated as harmonic, and no attempt was made to treat torsional modes in a more appropriate manner,[55] but the errors introduced by these approximations are expected to lie below the inherent error limits of the electronic structure calculations.

Atomic charges and sharing indices were computed by using PROAIMV[56] and AIM96.[57] The natural population analyses (NPA) and natural bond orbital (NBO) analyses were carried out with the Gaussian 94 package, which contains code implementing these methods as defined by Weinhold.[31,32] The wave functions were computed at the QCISD level,[58] which is known to minimize problems associated with spin contamination,[59] using the 6-311+G**(6D) basis set[60] and at the UMP2/6-31G* optimized geometries.[61]

The spin density distributions shown in Figure 5 were computed with the Gaussian 94 package and then plotted by using the programs of the CASGEN package developed at Yale University.[62] The difference density distributions shown in Figures 8 and 9 were both computed and plotted with the CASGEN package.

Acknowledgment. Financial support for this work was provided by Swarthmore College, the DuPont Chemical Company, the Camille and Henry Dreyfus Foundation (through the Faculty Start-up Grant Program for Undergraduate Institutions), and the Donors of the Petroleum Research Fund, administered by the American Chemical Society.[7] P.R.R. acknowledges the intellectual contributions of John Hartwig of the Yale University Department of Chemistry, whose interest in borane BDE's sparked this research project; of an anonymous referee for an earlier publication who suggested exploring BDE's of tetraco-

(52) Frisch, M. J.; Trucks, G. W.; Schlegel, H. B.; Gill, P. M. W.; Johnson, B. G.; Robb, M. A.; Cheeseman, J. R.; Keith, T.; Petersson, G. A.; Montgomery, J. A.; Raghavachari, K.; Al-Laham, M. A.; Zakrzewski, V. G.; Ortiz, J. V.; Foresman, J. B.; Cioslowski, J.; Stefanov, B. B.; Nanayakkara, A.; Challacombe, M.; Peng, C. Y.; Ayala, P. Y.; Chen, W.; Wong, M. W.; Andres, J. L.; Replogle, E. S.; Gomperts, R.; Gonzalez, C.; Martin, R. L.; Fox, D. J.; Binkley, J. S.; Defrees, D. J.; Baker, J.; Stewart, J. P.; Head-Gordon, M.; Gonzalez, C.; Pople, J. A. *Gaussian 94* (Revision C.2); Gaussian, Inc.: Pittsburgh, PA, 1995.

(53) Janz, G. J. *Thermodynamic Properties of Organic Compounds: Estimation Methods, Principles and Practice*, revised edition; Academic Press: New York, 1967.

(54) Rablen, P. R. *THERMO, version 1.0*; Yale University: New Haven, CT, 1993.

(55) Cf.: Wiberg, K. B.; Rablen, P. R.; Rush, D. J.; Keith, T. A. *J. Am. Chem. Soc.* **1995**, *117*, 4261−4270.

(56) Biegler-König, F. W.; Bader, R. F. W.; Tang, T.-H. *J. Comput. Chem.* **1982**, *3*, 317. Bader, R. F. W.; Tang, T.-H.; Tal, Y.; Biegler-König, F. W. *J. Am. Chem. Soc.* **1982**, *104*, 946−952.

(57) Keith, Todd A. *AIM96*; Yale University: New Haven, CT, 1996.

(58) Pople, J. A.; Head-Gordon, M.; Raghavachari, K. *J. Chem. Phys.* **1987**, *87*, 5968−5975.

(59) Chen, W.; Schlegel, H. B. *J. Chem. Phys.* **1994**, *101*, 5957−5968.

(60) McLean, A. D.; Chandler, G. S. *J. Chem. Phys.* **1980**, *72*, 5639−5648. Krishnan, R.; Binkley, J. S.; Seeger, R.; Pople, J. A. *J. Chem. Phys.* **1980**, *72*, 650−654.

(61) Head-Gordon, M.; Pople, J. A.; Frisch, M. J. *Chem. Phys. Lett.* **1988**, *153*, 503−506. Frisch, M. J.; Head-Gordon, M.; Pople, J. A. *Chem. Phys. Lett.* **1990**, *166*, 275−280. Frisch, M. J.; Head-Gordon, M.; Pople, J. A. *Chem. Phys. Lett.* **1990**, *166*, 281−289. Head-Gordon, M.; Head-Gordon, T. *Chem. Phys. Lett.* **1994**, *220*, 122−128.

(62) Hadad, C. M.; Rablen, P. R. *CASGEN package, version 1.0*; Yale University: New Haven, CT, 1992.

ordinate boron species in more detail; and of Brian Frink, who suggested some of the alternative bond dissociation pathways in Scheme 1. P.R.R. thanks Ahamindra Jain of the Swarthmore College Department of Chemistry and Kenneth Wiberg of the Yale University Department of Chemistry for helpful and stimulating discussions of the material described in this paper. P.R.R. is also grateful for access to a pre-release version of the AIM96 integration software package written by Todd Keith.[57]

Supporting Information Available: Table of absolute molecular energies in hartrees; optimized geometries of all species for which calculations were performed, in Z-matrix form; discussion of the effect of different definitions of atomic population on structural correlations; plot comparing BDE's with NPA spin densities; plot comparing NPA and AIM spin densities; table of NPA and AIM atomic populations; plot of B−H BDE versus change in BH_2 population; table of changes in NPA populations resulting from geometry modifications in the difference density calculations, and associated discussion; plot of B−H BDE versus change in B−X sharing index; plot of association enthalpy versus B−X sharing index for open-shell complexes; table of HOMO energies for Lewis bases, and associated discussion (80 pages). See any current masthead page for ordering and Internet access instructions.

JA970870P